Cancer Cell
Article

Hedgehog Signaling Restrains Bladder Cancer Progression by Eliciting Stromal Production of Urothelial Differentiation Factors

Kunyoo Shin,[1,4,9,10,*] Agnes Lim,[1,3,4,9] Chen Zhao,[1,2,4] Debashis Sahoo,[1,5] Ying Pan,[6,8] Edda Spiekerkoetter,[7] Joseph C. Liao,[6,8] and Philip A. Beachy[1,2,3,4,*]
[1]Institute for Stem Cell Biology and Regenerative Medicine
[2]Department of Biochemistry
[3]Department of Developmental Biology
[4]Howard Hughes Medical Institute
[5]Department of Pathology
[6]Department of Urology
[7]Department of Medicine, Vera Moulton Wall Center for Pulmonary Vascular Disease, Cardiovascular Institute
Stanford University School of Medicine, Stanford, CA 94305, USA
[8]Veterans Affairs Palo Alto Health Care System, Palo Alto, CA 94304, USA
[9]Co-first author
[10]Present address: Department of Cell, Developmental and Cancer Biology and Department of Urology, School of Medicine, Oregon Health & Science University, Portland, OR 97239, USA
*Correspondence: shink@ohsu.edu (K.S.), pbeachy@stanford.edu (P.A.B.)
http://dx.doi.org/10.1016/j.ccell.2014.09.001

SUMMARY

Hedgehog (Hh) pathway inhibitors are clinically effective in treatment of basal cell carcinoma and medulloblastoma, but fail therapeutically or accelerate progression in treatment of endodermally derived colon and pancreatic cancers. In bladder, another organ of endodermal origin, we find that despite its initial presence in the cancer cell of origin *Sonic hedgehog* (*Shh*) expression is invariably lost during progression to invasive urothelial carcinoma. Genetic blockade of stromal response to Shh furthermore dramatically accelerates progression and decreases survival time. This cancer-restraining effect of Hh pathway activity is associated with stromal expression of BMP signals, which stimulate urothelial differentiation. Progression is dramatically reduced by pharmacological activation of BMP pathway activity with low-dose FK506, suggesting an approach to management of human bladder cancer.

INTRODUCTION

Postnatal Hedgehog (Hh) signaling functions in regulation of stem cell physiology and tissue regeneration (Ahn and Joyner, 2005; Lai et al., 2003; Palma et al., 2005; Shin et al., 2011; Taipale and Beachy, 2001). Following bacterial injury of the bladder, for example, *Sonic hedgehog* (*Shh*) produced in cells of the basal urothelium elicits production of secreted factors from stromal cells, which in turn stimulate proliferation and differentiation of urothelial cells. This epithelial/stromal feedback leads to regeneration of the urothelium and restoration of its normal function. In this regenerative response to murine urinary tract infection, the *Shh*-expressing basal cells function as stem cells by proliferating and supplying the progenitor cells that give rise to differentiated cells which ultimately replenish the injured urothelium (Shin et al., 2011).

These *Shh*-expressing basal stem cells also give rise to invasive urothelial carcinoma in a murine chemical carcinogenesis model utilizing the procarcinogen N-butyl-N-4-hydroxybutyl nitrosamine (BBN) (Shin et al., 2011, 2014). Nitrosamines are potent carcinogens present in cigarette smoke, the most important risk factor in human bladder cancer, and BBN specifically induces advanced bladder cancer in many experimental animals (Bryan, 1977, 1983; Nagao et al., 1977; Shin et al., 2014). In our previous

Significance

Aberrant Hedgehog (Hh) pathway activation has been associated with a wide range of cancers, yet clinical trials involving the treatment of solid tumors with Hh pathway inhibitors have yielded disappointing results. Our findings that loss of human urothelial *SHH* expression accompanies progression to invasive urothelial carcinoma, and that ablation of Shh response in stromal cells can accelerate progression in mice shows both that stromal signaling has a beneficial role in restraining progression of urothelial carcinoma and that pharmacological blockade of Hh signaling is contra-indicated in this disease. A favorable effect of BMP pathway activation with low-dose FK506 suggests a clinical approach to control of progression in the 70%–80% of patients that present with noninvasive urothelial carcinoma at initial diagnosis.

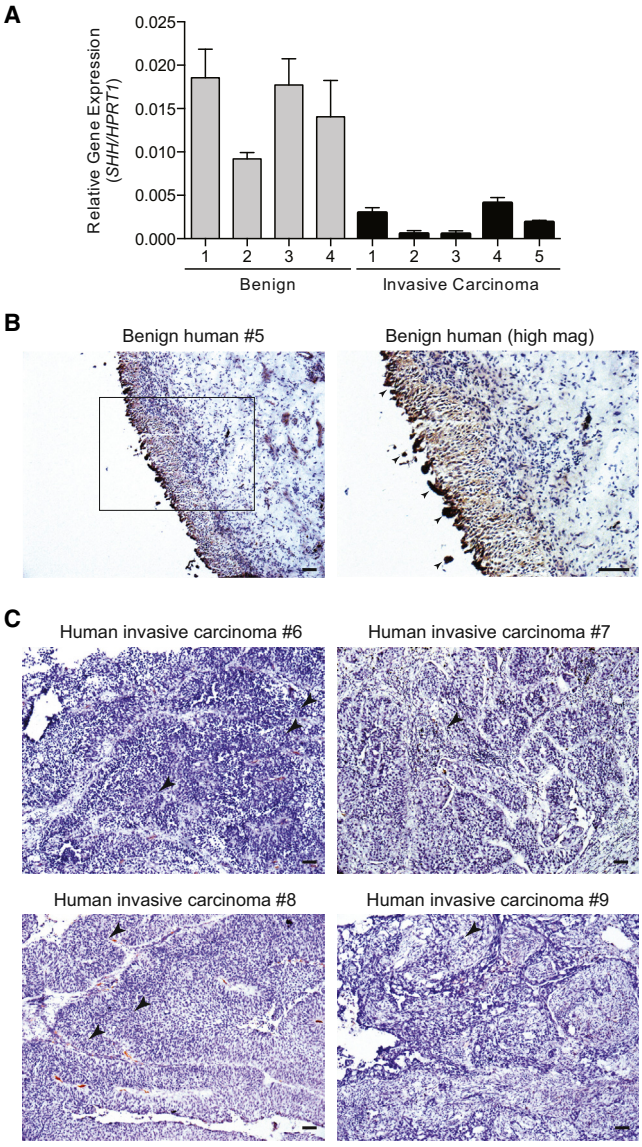

Figure 1. Absence of *Sonic Hedgehog* Expression in Human Invasive Bladder Carcinoma

(A) Real time quantitative PCR measurement of *SHH* expression in benign urothelium and invasive urothelial carcinoma tissues. Data are presented as mean ± SEM, n = 3 technical replicates for each independent sample.

(B) Benign human urothelium immunostained for Shh and counterstained with hematoxylin. Arrowheads in the boxed area enlarged on the right indicate nonspecific staining of dying cells being sloughed off into the lumen.

(C) Human invasive urothelial carcinoma samples from four patients immunostained for Shh and counterstained with hematoxylin. Arrowheads indicate regions of Shh reactivity within tumor vasculature. Scale bars represent 50 μm. Sample numbers correspond to those in Table S1.

See also Figure S1 and Table S1.

work, murine exposure to BBN reliably induced a premalignant lesion histologically indistinguishable from human urothelial carcinoma in situ (CIS) by 3–4 months of exposure, with invasive carcinoma developing by 5–6 months (Shin et al., 2014). BBN exposure thus provides a clinically relevant experimental model of human bladder carcinogenesis with a defined course of progression to invasive carcinoma, with no prior bias regarding genetic pathway or cell type.

We found in this model that marking of *Shh*-expressing basal cells invariably marks tumors, whereas ablation of these cells decisively abrogates tumor formation. Surprisingly, although this combination of positive and negative evidence clearly demonstrates that basal urothelial stem cells expressing *Shh* are the exclusive cell of origin for invasive bladder cancer, expression of *Shh* is lost by the time invasive carcinomas are formed (Shin et al., 2011, 2014). A possible explanation for this observation is that loss of *Shh* expression may somehow promote tumor progression. This effect, however, would represent a novel protective role for Hh pathway activity, as mutational activation of the Hh pathway is causative in the primary cells of basal cell carcinoma and medulloblastoma (Hahn et al., 1996; Johnson et al., 1996; Teglund and Toftgård, 2010), and ligand-dependent pathway activity in stroma has been thought to promote growth of pancreatic cancer (Olive et al., 2009; Yauch et al., 2008). To elucidate the role of Hh signaling in bladder carcinogenesis, we have examined *SHH* expression and signaling in benign and malignant human bladder and have investigated the role and mechanism of Hh signaling in the murine BBN model.

RESULTS

Absence of *Sonic Hedgehog* Expression in Human Invasive Urothelial Carcinoma

Having previously established the absence of *Shh* expression in murine invasive urothelial carcinoma (Shin et al., 2014), we compared the expression of *SHH* mRNA in human benign urothelium to that in five muscle-invasive urothelial carcinoma samples, with histological confirmation by hematoxylin and eosin (H&E) staining of tissue sections (Figure S1A available online, patient information in Table S1). We found that all five invasive carcinoma samples examined showed a marked decrease in *SHH* expression (Figure 1A), consistent with our previous work in murine invasive urothelial carcinoma. To confirm and extend these results, we performed immunohistochemistry (IHC) for the expression of Shh protein in additional human invasive urothelial carcinoma samples using an antibody that specifically detects Shh, as validated by IHC of embryonic murine tissues in which the expression pattern of Shh is well established (Roelink et al., 1995) (Figure S1B). We found high levels of Shh protein in human benign bladder urothelium (Figures 1B and S1C), but little if any detectable Shh in the primary cancer cells of all eight invasive carcinomas examined (Figures 1C and S1C). We note that although Shh immunoreactivity was absent in cells of the carcinoma, it was present within the tumor vasculature, and this may account for the low level of *SHH* mRNA detected in the carcinoma samples by RT-PCR. In addition to *SHH*, we also found a decrease in the expression of Hh pathway target genes *GLI1* and *PTCH1* in all five invasive carcinoma samples (Figure S1D) indicating that Hh pathway activity is reduced in response to the decreased expression of ligand.

Genetic Ablation of Hedgehog Response Accelerates Bladder Carcinogenesis

Given the consistent absence of *SHH* expression in invasive urothelial carcinoma, we tested the possibility that loss of Hh

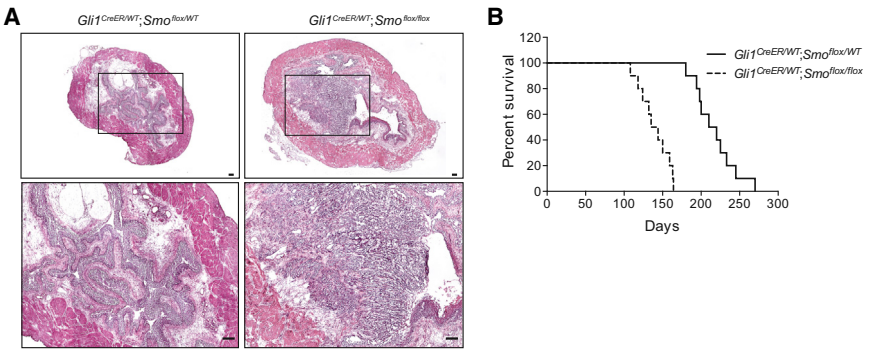

Figure 2. Genetic Ablation of Hedgehog Response Accelerates Bladder Carcinogenesis

(A) H&E stains of bladder sections from mice treated with TM, then exposed to BBN for 3 months. Magnified views (lower panels) of boxed regions confirm the presence (*Gli1*$^{CreER/WT}$;*Smo*$^{flox/flox}$, mice with homozygous loss of *Smo*) or absence (*Gli1*$^{CreER/WT}$;*Smo*$^{flox/WT}$, heterozygous control mice) of invasive carcinoma. Scale bars represent 50 μm. (B) Kaplan-Meier survival curve of *Gli1*$^{CreER/WT}$;*Smo*$^{flox/flox}$ and *Gli1*$^{CreER/WT}$;*Smo*$^{flox/WT}$ mice (n = 10 in each group) injected with TM, exposed to BBN, and euthanized when they became morbidly ill. Animals with homozygous loss of *Smo* survived a median of 140 days, as compared to 215 days for *Smo* heterozygous control animals ($p < 0.0001$, as determined by the log-rank test).

signaling may accelerate tumor growth and progression, using exposure of mice to BBN in drinking water as a model of bladder carcinogenesis with a defined course of progression to invasive carcinoma. In this model, the use of chemical rather than genetically induced carcinogenesis permits the unencumbered use of genetic methods to investigate the biology of the tumor. We previously made use of genetic marking to establish that the *Shh*-expressing basal stem cell is the cancer cell of origin and to investigate the tissue dynamics of invasive bladder cancer progression (Shin et al., 2011, 2014); here we use genetic methods to probe the role of Hh signaling during carcinogenesis.

As previously established, *Shh* expression occurs constitutively in basal cells of the urothelium and response to the signal, as manifested by expression of *Gli1*, is restricted to stromal cells (Shin et al., 2011). To genetically inactivate stromal Hh response, we injected tamoxifen (TM) into mice expressing CreER under control of the *Gli1* promoter and carrying homozygous floxed alleles of the essential Hh pathway transductory component *Smoothened* (*Smo*) (*Gli1*$^{CreER/WT}$;*Smo*$^{flox/flox}$). Ablation of *Smo* in this manner will block Hh response in stromal cells undergoing Hh response under baseline conditions, prior to BBN exposure. In mice thus treated, we found that invasive carcinomas appeared as early as 3 months after initiation of BBN exposure (Figure 2A, right panels), a time at which control animals were just beginning to develop CIS-like lesions (Figure 2A, left panels). Furthermore, these mice survived a median of 140 days, as compared to 215 days for *Smo* heterozygous control animals (Figure 2B), indicating that wild-type (WT) *Smo* function confers a 53% survival benefit. Genetic ablation of Hh response in bladder stroma thus significantly accelerates the progression of BBN-induced bladder cancer.

This result suggests a possible basis for the prevalence of invasive carcinomas lacking *Shh* expression: given that uniform loss of Hh response throughout the stroma accelerates cancer growth, it seems reasonable that loss of *Shh* expression from a clone of premalignant cells in a CIS lesion may confer a local growth advantage by reducing Hh pathway response in neighboring stroma, ultimately leading to preferential expansion of such clones of cells during progression to advanced invasive urothelial carcinomas.

Reduced Expression of Differentiation Factors in *Smoothened*-Ablated Mice

The consistent loss or attenuation of *Shh* expression in the later stages of tumor progression and the experimental acceleration of tumor progression with genetic ablation of *Smo* function in Hh-responsive stromal cells together suggest that secreted stromal factors induced by Hh signaling restrain the formation of aggressive tumors. To identify Hh-regulated molecular pathways involved in delaying tumor formation, we performed gene expression profiling on bladder samples from *Gli1*$^{CreER/WT}$;*Smo*$^{flox/flox}$ and *Gli1*$^{CreER/WT}$;*Smo*$^{flox/WT}$ mice. Following TM injection, mice were exposed to BBN for 2 months prior to gene expression analyses (Figure S2A). The 2-month time point was chosen in order to detect molecular changes that are present early in the tumor formation process, before overt histological differences can be seen, as these early molecular changes are likely to drive the cellular processes responsible for later phenotypic differences. Indeed, bladders from BBN-exposed mice of both genotypes were histologically identical at this 2-month time point (Figure S2B), and did not display differences in epithelial:stromal cell ratios (Figure S2C) or in the density of vascular elements (Figure S2D).

Comparison of the gene expression profiles revealed that 468 genes were at least 2-fold downregulated in bladder samples from *Gli1*$^{CreER/WT}$;*Smo*$^{flox/flox}$ mice exposed to BBN ($p < 0.01$); gene ontology analysis indicated an enrichment of genes involved in developmental processes and cell differentiation in this list (Table S2). The apparent downregulation of cell differentiation genes in TM-treated *Gli1*$^{CreER/WT}$;*Smo*$^{flox/flox}$ mice suggests the possibility that accelerated cancer progression with loss of Hh pathway activity is due to decreased expression of differentiation-promoting factors that may increase the pool of primitive cells with the potential to progress to invasive carcinoma. Supporting this hypothesis, we found that *Uroplakin* gene expression, which is indicative of urothelial differentiation, is significantly decreased in *Smo*-ablated mouse bladders (Figure S2E). As decreased Hh pathway activity, occurring in stroma, must affect tumor-forming urothelial cells, we focused on those cell differentiation genes (Table 1) that encode secreted proteins involved in cell signaling (Figure 3A). Bone morphogenic protein 4 (Bmp4) and Bmp5 (Bragdon et al., 2011) are particularly of interest because: (1) Bmp4 has been shown to promote terminal

Table 1. Genes Downregulated in *Gli1*$^{CreER/WT}$;*Smo*$^{flox/flox}$ Mouse Bladders, following 2 Months of N-butyl-N-4-hydroxybutyl Nitrosamine Treatment, Involved in Cell Differentiation—GO:0030154

Accession Number	Symbol	Gene Name	Fold Change	p Value
NM_007555	*Bmp5*	bone morphogenetic protein 5	−8.0	1.59E-03
NM_027852	*Rarres2*	retinoic acid receptor responder (tazarotene induced) 2	−6.5	1.31E-06
NM_024406	*Fabp4*	fatty acid binding protein 4	−6.2	4.44E-03
NM_009605	*Adipoq*	adiponectin, C1Q, and collagen domain containing	−6.0	5.17E-05
NM_007554	*Bmp4*	bone morphogenetic protein 4	−5.3	1.19E-04
NM_177708	*Rtn4rl1*	reticulon 4 receptor-like 1	−5.0	4.92E-03
NM_001164035	*Nft3*	neurotrophin 3	−4.8	2.38E-03
NM_009122	*Satb1*	special AT-rich sequence binding protein 1	−4.0	6.07E-03
NM_031166	*Id4*	inhibitor of DNA binding 4	−3.8	8.97E-03
NM_022984	*Retn*	resistin	−3.8	4.21E-03
NM_025943	*Dzip1*	DAZ interacting protein 1	−3.7	1.35E-03
NM_173004	*Cntn4*	contactin 4	−3.6	4.23E-03
NM_011255	*Rbp4*	retinol binding protein 4, plasma	−3.6	8.99E-03
NM_001001309	*Itga8*	integrin alpha 8	−3.6	1.11E-03
NM_009204	*Slc2a4*	solute carrier family 2 (facilitated glucose transporter), member 4	−3.6	9.72E-03
NM_009152	*Sema3a*	sema domain, immunoglobulin domain, short basic domain, secreted, (semaphorin) 3A	−3.4	5.00E-03
NM_009365	*Tgif1i1*	transforming growth factor beta 1 induced transcript 1	−3.4	1.75E-03
NM_001111027	*Runx1t1*	Runt-related transcription factor 1; translocated to, 1 (cyclin D-related)	−3.4	2.46E-03
NM_172621	*Clic5*	chloride intracellular channel 5	−3.4	1.91E-03
NM_175260	*Myh10*	myosin, heavy polypeptide 10, nonmuscle	−3.2	6.48E-03
NM_015753	*Zeb2*	zinc finger E-box binding homeobox 2	−3.1	2.77E-03
NM_008086	*Gas1*	growth arrest specific 1	−3.1	8.17E-05
NM_010681	*Lama4*	laminin, alpha 4	−3.1	3.14E-03
NM_027280	*Nkd1*	naked cuticle 1 homolog (Drosophila)	−3.1	7.01E-03
NM_010518	*Igfbp5*	insulin-like growth factor binding protein 5	−3.0	3.68E-03
NM_021339	*Cdon*	cell adhesion molecule-related/downregulated by oncogenes	−2.9	3.60E-03
NM_025282	*Mef2c*	myocyte enhancer factor 2C	−2.8	5.03E-03
NM_010280	*Gfra3*	glial cell line derived neurotrophic factor family receptor alpha 3	−2.8	8.04E-04
NM_177089	*Tacc1*	transforming, acidic coiled-coil containing protein 1	−2.7	2.76E-03
NM_001081106	*Cytl1*	cytokine-like 1	−2.7	1.88E-04
NM_001102400	*Dab2*	disabled homolog 2 (Drosophila)	−2.7	4.71E-03
NM_011614	*Tnfsf12*	tumor necrosis factor (ligand) superfamily, member 12	−2.6	2.49E-03
NM_025891	*Smarcd3*	SWI/SNF related, matrix associated, actin dependent regulator of chromatin, subfamily d, member 3	−2.6	8.69E-04
NM_011129	*Sept4*	septin 4	−2.5	3.40E-03
NM_001083334	*Bin1*	bridging integrator 1	−2.5	3.37E-03
NM_009153	*Sema3b*	sema domain, immunoglobulin domain, short basic domain, secreted, (semaphorin) 3B	−2.2	4.37E-06
NM_172506	*Boc*	biregional cell adhesion molecule-related/downregulated by oncogenes (Cdon) binding protein	−2.2	7.64E-03
NM_001159382	*Gjc1*	gap junction protein, gamma 1	−2.2	1.50E-03
NM_023328	*Agtpbp1*	ATP/GTP binding protein 1	−2.1	5.46E-03
NM_008493	*Lep*	leptin	−2.1	6.27E-03
NM_001085370	*Speg*	SPEG complex locus	−2.1	9.46E-03
NM_001198571	*Abi2*	Abl-interactor	−2.0	4.28E-03

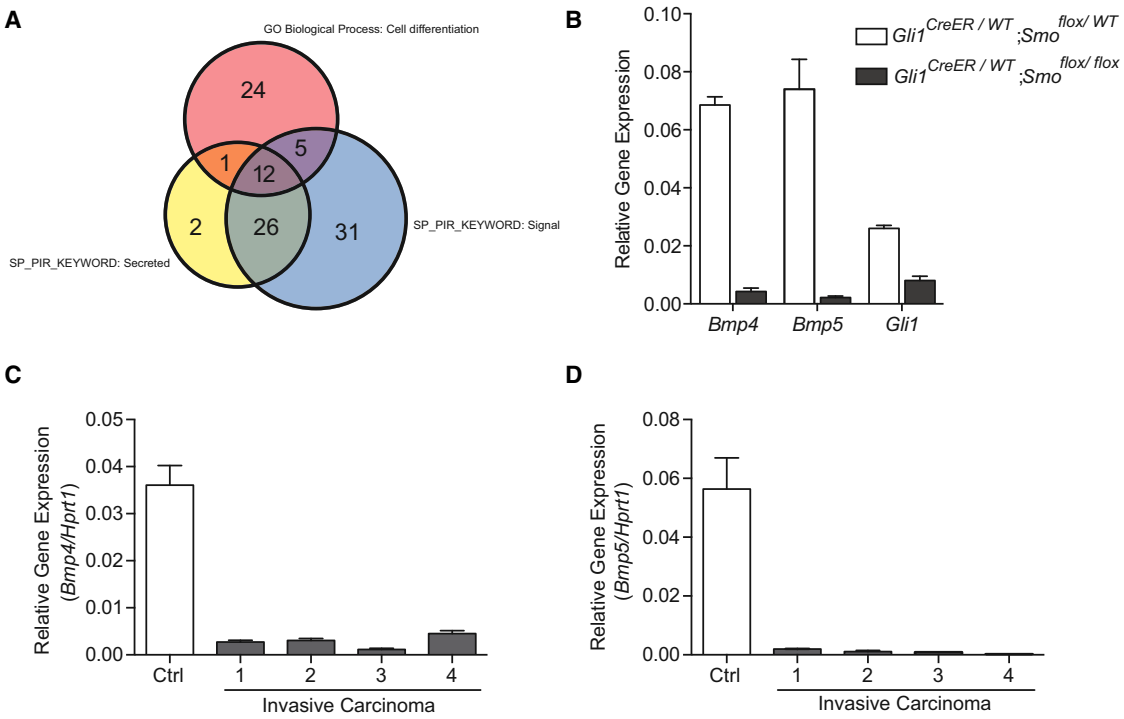

Figure 3. Reduced Expression of Differentiation Factors in *Smoothened*-Ablated Mice

(A) Comparison of gene expression profiles revealed 468 genes downregulated by at least 2-fold in *Gli1*$^{CreER/WT}$;*Smo*$^{flox/flox}$ as compared to *Gli1*$^{CreER/WT}$;*Smo*$^{flox/WT}$ bladder samples ($p < 0.01$). Gene ontology analysis indicated an enrichment of genes involved in cell differentiation. Additional functional annotation of the downregulated genes showed enrichment in the SP and Protein Information Resource Keywords (SP_PIR_KEYWORD) "Signal" and "Secreted." The Venn diagram shows the number of overlapping genes in each of the three categories, with 12 genes that encode secreted proteins involved in cell signaling and differentiation.

(B) Expression in bladders of *Gli1*$^{CreER/WT}$;*Smo*$^{flox/flox}$ as compared to *Gli1*$^{CreER/WT}$;*Smo*$^{flox/WT}$ mice of *Bmp4* (16-fold decrease, $p < 0.0001$), *Bmp5* (34-fold decrease, $p < 0.001$), and *Gli1* (3.2-fold decrease, $p < 0.0001$). Mice were injected with TM just prior to 2 months of BBN exposure.

(C and D) Expression in four bladders from BBN-exposed mice (6 months) with invasive carcinoma of *Bmp4* ($p < 0.001$) and *Bmp5* ($p < 0.001$) as compared to a control bladder (Ctrl) with no BBN exposure. Data are presented as mean ± SEM, and significance was calculated by an unpaired Student's t test. n = 3 technical replicates, and the entire experiment was repeated three times.

See also Figure S2 and Table S2.

differentiation of bladder urothelium (Mysorekar et al., 2009); (2) some Bmp genes are known to be directly regulated by Hh pathway activity (Kawai and Sugiura, 2001; Roberts et al., 1995); and (3) Bmp signaling plays a role in the differentiation of tissues in other organs such as lungs (Weaver et al., 1999) and heart (Schultheiss et al., 1997).

To confirm decreased *Bmp4* and *Bmp5* expression, we carried out quantitative RT-PCR with samples from the bladders of TM-injected *Gli1*$^{CreER/WT}$;*Smo*$^{flox/flox}$ and *Gli1*$^{CreER/WT}$;*Smo*$^{flox/WT}$ mice exposed to BBN for 2 months. Attenuation of Hh pathway activity was verified by a reduction in the expression of *Gli1*, a transcriptional target of the pathway, and this was correlated with a sharp reduction in the levels of *Bmp4* and *Bmp5* (Figure 3B). We further examined *Bmp4* and *Bmp5* mRNA in WT mice exposed to BBN for 6 months and found that expression of *Bmp4* and *Bmp5* was greatly reduced in invasive carcinoma as compared to control bladders from mice without exposure to BBN (Figures 3C and 3D). This was accompanied by a decrease in the expression of Hh target genes *Gli1* and *Ptch1* (Figure S2F) and Bmp target genes *Id1*, *Id2*, *Id3,* and *Cdkn1b* (Figure S2G). These results suggest that decreased *Bmp* expression resulting from loss of Hh signaling may account for the accelerated rate of tumor progression observed in mice with ablated *Smo* function (Figure 2A).

Stromal Hedgehog Response Regulates Expression of Human *BMP4* and *BMP5* Genes

To determine whether Hh signaling regulates expression of *BMP4* and *BMP5* in human bladder, we first examined the expression of Hh pathway components in primary human bladder fibroblasts and epithelial cells. Consistent with immunostaining for Shh using benign bladder sections (Figures 1B and S1C), we found that *SHH* is expressed in primary cultures of human bladder urothelial cells (Figure S3A), consistent with our findings in the mouse (Shin et al., 2011). To evaluate response to the Hh signal, we treated cultured human bladder stromal and urothelial cells with ShhN protein or with the chemical pathway agonist SAG (Chen et al., 2002b). Hh pathway activation, as judged by an increase in *GLI1* expression, only occurred in cultured stromal cells (Figure 4A), and this effect was reversed by addition of the pathway antagonist cyclopamine (Chen et al., 2002a; Cooper et al., 1998), suggesting that Hh signaling in

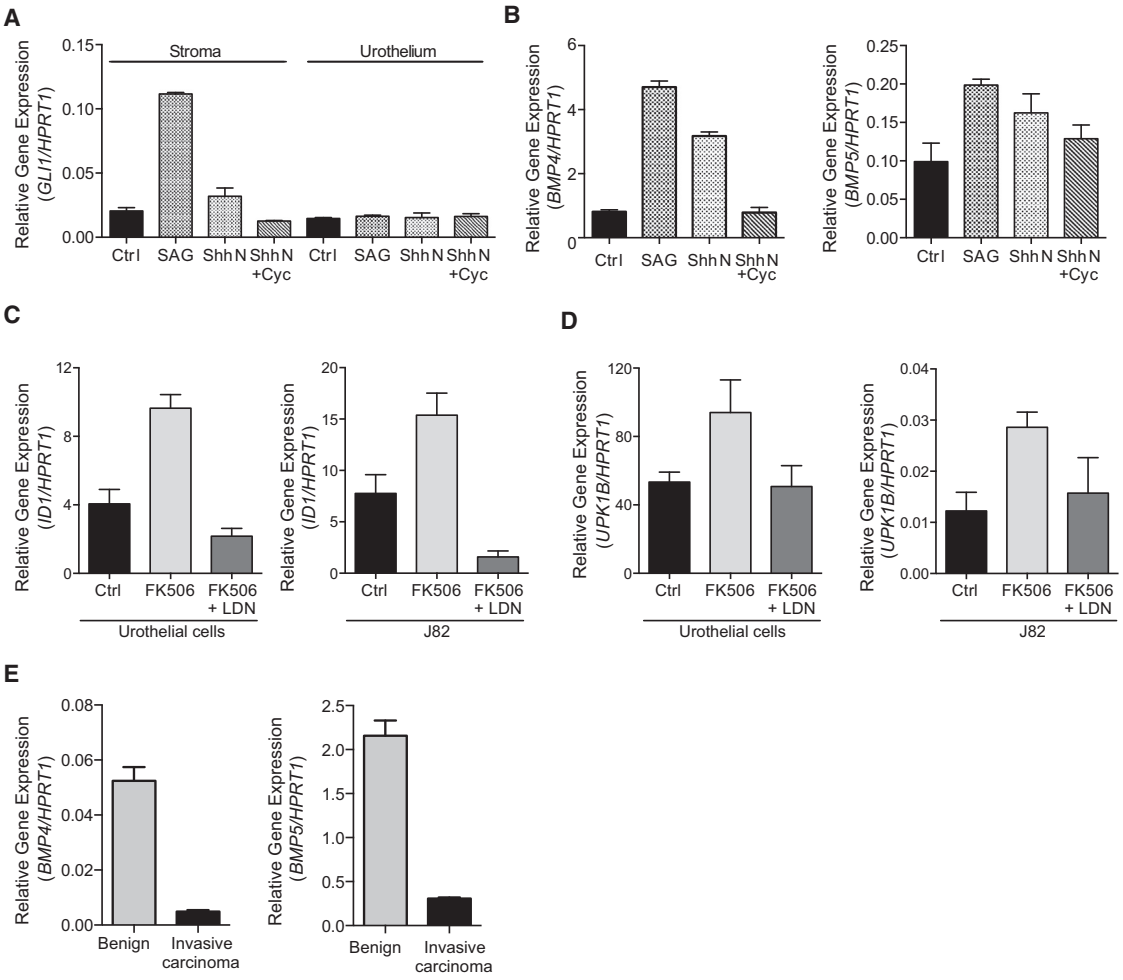

Figure 4. Stromal Hedgehog Response Regulates Expression of Human *BMP4* and *BMP5* Genes

(A) Expression of *GLI1* in primary human bladder stromal cells treated with SAG (5.4-fold increase, $p < 0.001$), ShhN (1.6-fold increase, $p < 0.05$), and ShhN + cyclopamine (Cyc) (no statistically significant change) as compared to unstimulated Ctrl stromal cells or in primary human bladder urothelial cells as compared to Ctrl urothelial cells (no statistically significant change with any treatment).

(B) *BMP4* and *BMP5* expression in primary human bladder stromal cells treated with SAG (*BMP4*: 5.8-fold increase, $p < 0.001$ and *BMP5*: 2-fold increase, $p < 0.01$), ShhN (*BMP4*: 3.9-fold increase, $p < 0.001$ and *BMP5*: 1.6-fold increase, $p < 0.05$), and ShhN + Cyc (no statistically significant change) as compared to unstimulated Ctrl cells.

(C) Expression of BMP target gene *ID1* in cells treated with BMP agonist FK506 as compared to the DMSO vehicle Ctrl (2.4-fold increase in urothelial cells, $p < 0.01$ and 2-fold increase in J82 urothelial carcinoma cells, $p < 0.01$) or as compared to cells treated with FK506 after preincubation with the BMP inhibitor LDN-193189 (LDN)(4.5-fold increase in urothelial cells, $p < 0.0001$ and 10-fold increase in J82 cells, $p < 0.001$).

(D) Expression of the urothelial differentiation marker *UPK1B* in cells treated with FK506 as compared to DMSO Ctrl (3.2-fold increase in urothelial cells, $p < 0.01$ and 2.3-fold increase in J82 cells, $p < 0.01$) or as compared to cells treated with FK506 after preincubation with LDN (2.7-fold increase in urothelial cells, $p < 0.01$ and 1.8-fold increase in J82 cells, $p < 0.05$).

(E) Expression in human invasive urothelial carcinoma as compared to benign bladder tissues of *BMP4* (11-fold decrease, $p < 0.001$) and *BMP5* (7-fold decrease, $p < 0.001$). Data are presented as mean ± SEM, and significance was calculated by an unpaired Student's t test. n = 3 technical replicates, and the entire experiment was repeated three times.

See also Figure S3.

human bladder mirrors that in the mouse, with epithelial expression of Hh ligand and signal response restricted to stroma (Shin et al., 2011). Concomitant with the increase in *GLI1* mRNA upon stimulation of the cultured human bladder stromal fibroblasts, we noted an increase in levels of *BMP4* and *BMP5* transcripts (Figure 4B). These data suggest that stromal cells in human bladder, like those in the mouse, respond to Hh ligand stimulation with increased transcription of *BMP4* and *BMP5*.

As Bmp4 and Bmp5 secreted from stromal cells have the potential to act on urothelium, we examined the response of human urothelial cells and urothelial carcinoma cells to BMP pathway activation. To pharmacologically activate the BMP pathway, we selected FK506, a drug that has long been used in transplant patients for its immunopsuppressive effects. FK506 binds FKBP12 and inhibits calcineurin, thus preventing activation of NFAT and transcription of cytokines essential for immune

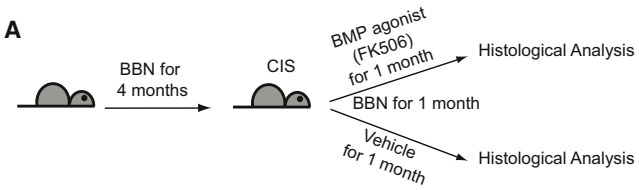

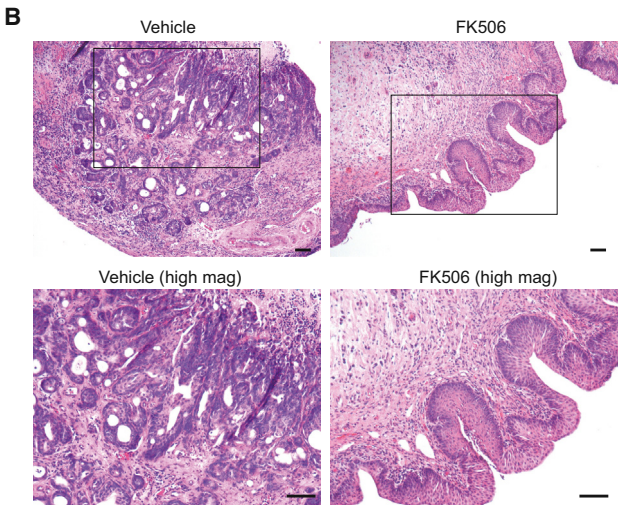

C

	Carcinogen treated	Drug	Starting/ending time of drug treatment	Total number of mice treated with drug	Number of mice that developed invasive tumors
Group 1	BBN	Vehicle	4mo/5mo	9	7
Group 2	BBN	FK506	4mo/5mo	10	0

Figure 5. Pharmacological Activation of Bone Morphogenic Protein Signaling In Vivo Impedes Tumor Progression

(A) Schematic diagram of experimental strategy used to analyze the effect of BMP pathway activation on bladder cancer progression. Mice exposed to BBN for 4 months were treated with the BMP agonist FK506 or a vehicle control for a month with continued BBN exposure before histopathological analysis of the bladders.

(B) Bladder sections from mice exposed to BBN for 5 months with 1 month of treatment with FK506 or a vehicle control were stained with H&E. Lower panels show magnified views of the regions highlighted by boxes in upper panels. Scale bars represent 50 μm.

(C) Results obtained from the treatment of mice exposed to BBN with FK506 or a vehicle control are summarized. See also Figure S4.

response (Crabtree and Schreiber, 2009; Liu et al., 1991). Of particular interest here, we recently showed that FK506 also causes dissociation of FKBP12 from Type 1 BMP receptors, thus activating the BMP pathway; this occurs at concentrations below those required for immunosuppression, and FK506 at these lower doses has proven to be effective upon systemic administration in animal models of pulmonary arterial hypertension, which is causally associated with a deficiency of BMP pathway activity (Spiekerkoetter et al., 2013).

The treatment of cultured primary urothelial cells with FK506 induced expression of the BMP target gene *ID1* (Miyazono and Miyazawa, 2002; Miyazono et al., 2005; Samanta and Kessler, 2004); this activation was blocked by combined treatment with FK506 and the potent and specific BMP inhibitor LDN-193189 (Figure 4C) (Cuny et al., 2008; Yu et al., 2008), thereby confirming in our system that FK506 acts via BMP pathway activation. Treatment of cultured urothelial cells with FK506 also induced expression of the uroplakin genes *UPK1B, UPK2*, and *UPK3A*, indicative of urothelial cell differentiation and consistent with the previously reported role of BMP pathway activity in promoting urothelial differentiation in vivo (Mysorekar et al., 2009); again, this differentiation-inducing effect of FK506 treatment was blocked by combined treatment with LDN-193189 (Figures 4D and S3B). Similar results were obtained using the urothelial carcinoma cell line J82 (O'Toole et al., 1978) (Figures 4C and 4D).

These findings suggest a reciprocal epithelial-stromal signal feedback loop in which Shh secreted by the urothelium activates Hh response in bladder stromal cells, resulting in stromal expression of *BMP4* and *BMP5*, which in turn signal back to the urothelium to induce differentiation. Loss of *Shh* expression in human invasive carcinomas, as noted previously (Figure 1A), would be expected to disrupt this signal feedback; this expectation was confirmed by a dramatic reduction of *BMP4* and *BMP5* expression in human invasive urothelial carcinoma as compared to benign bladder (Figure 4E), as well as a reduction in expression of BMP target genes *ID1*, *ID2*, *ID3*, *ID4*, and *CDKN1B* (Figure S3C).

Pharmacological Activation of the Bone Morphogenic Protein Pathway Impedes Tumor Progression

To investigate the role of Bmp pathway activity in bladder tumor progression and to test the possibility that Bmp pathway activation might impede tumor progression by stimulating urothelial differentiation, we exposed mice to BBN for 4 months, then initiated treatment with FK506 for another month at concentrations below those required for its immunosuppressant effects (Spiekerkoetter et al., 2013) while also continuing exposure to BBN (Figure 5A). Bmp pathway activity in these mice was confirmed by increased expression of Bmp pathway targets, whereas unchanged expression of target genes in the calcineurin/NFAT pathway indicates minimal immunosuppressive activity (Figures S4A–S4C). We have previously noted that mice exposed to BBN for 4 months develop premalignant lesions indistinguishable from human CIS, but not invasive carcinoma, which requires further BBN exposure (Shin et al., 2014). In our control group, continuation of BBN exposure for a total of 5 months resulted in the development of invasive carcinoma in seven of nine mice. For the cohort of ten mice treated with FK506 during the final month, however, no invasive carcinoma was observed (Figures 5B, 5C, and S4D), suggesting that activation of Bmp pathway activity may impede progression if treatment occurs prior to formation of invasive carcinoma.

Large-Scale Transcriptional Profiling Suggests Loss of *Sonic Hedgehog*/Bone Morphogenic Protein Signaling in Invasive Human Bladder Cancers

Consistent with our finding of a functional role for loss of *Shh* expression in progression to invasive urothelial carcinoma, a previous RT-PCR analysis of human urothelial carcinomas at advanced stages also showed low or undetectable expression of *SHH* mRNA (Thievessen et al., 2005). In addition, our analysis (Figure 6) of data from recently published large-scale studies of gene expression in human invasive carcinoma also supports the loss of SHH and BMP signaling in invasive human urothelial

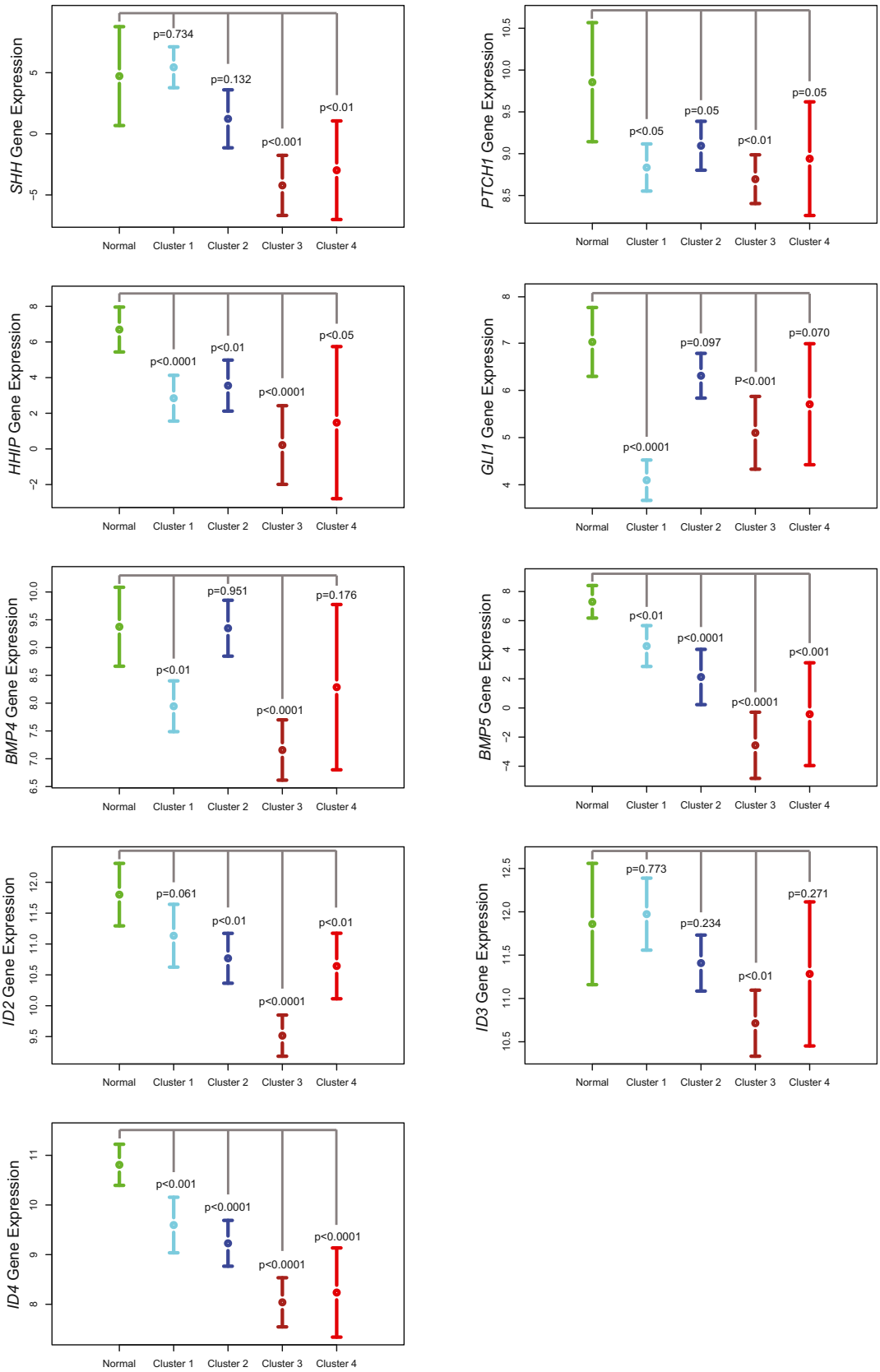

(legend on next page)

carcinoma (Cancer Genome Atlas Research Network, 2014; Choi et al., 2014). In this work, most human muscle-invasive urothelial carcinomas were subdivided into three major subtypes: papillary, luminal, and basal (Cancer Genome Atlas Research Network, 2014; Choi et al., 2014). Based on the level of expression of characteristic markers of basal versus luminal character, the invasive urothelial carcinomas produced in our BBN model are most similar to the basal subtype of human urothelial carcinoma (Figure S5A), which is the most aggressive form of bladder cancer and has a lower median overall survival than the other subtypes (Choi et al., 2014).

As the The Cancer Genome Atlas (TCGA) study also contains expression data for normal bladder, we can ask whether our findings of reduced *SHH* expression in invasive carcinoma relative to benign tissue are confirmed in human samples. A potential caveat of such a comparison is that the TCGA study only required that tumor nuclei constitute at least 60% of all nuclei in order for a sample to be included (Cancer Genome Atlas Research Network, 2014), whereas we used carefully selected samples exclusively containing tumor tissue in our study. Contamination with adjacent *SHH*-expressing benign tissue thus could confound conclusions from the TCGA data regarding *SHH* expression. Indeed, we have found that contamination of human invasive carcinoma samples with adjacent benign tissue leads to detection of higher *SHH* expression (Figures S5B and S5C).

We nevertheless found in the cluster 3 (basal) subtype of the TCGA study, which closely resembles the carcinoma subtype induced in our murine BBN model, that *SHH* mRNA was significantly reduced (500–1,000-fold or more; $p < 0.001$), as were its targets *PTCH1*, *GLI1*, *HHIP, BMP4*, *BMP5*, and the BMP targets *ID2*, *ID3*, and *ID4*. Given the magnitude of reduced expression for all these genes and the high degree of statistical significance (p ranged from < 0.01 to <0.001), these human data for the most aggressive basal subtype of invasive urothelial carcinoma (cluster 3) are fully consistent with our findings in the murine BBN model that loss of Hh expression and consequent decreased expression of BMP signals and downstream targets are an essential feature of urothelial carcinoma progression.

Expression of *SHH*, *BMP*, and their targets was also reduced in the other three subtypes of human invasive urothelial carcinoma, and statistical significance for these reductions was achieved in six of nine, five of nine, and six of nine of the genes analyzed for clusters 1, 2, and 4, respectively. The less uniform significance of the TCGA data for reduced expression of SHH/BMP genes in clusters 1, 2, and 4 may be due to greater contamination by benign epithelial tissues, whose presence could cause underestimation of the loss of epithelial SHH and stromal BMP. Such contamination likely is less of a factor for the more aggressive basal subtype (cluster 3), which would be expected to yield purer tumor samples due to faster growth and consequent crowding out of benign tissues. Alternatively, it may be possible that expression of differentiation-associated biomarkers in some luminal subtype carcinomas within clusters 1 and 2 may result from development of invasive properties while retaining a partial response to *SHH*/*BMP*.

A Model for Bladder Cancer Progression

Our observations together support the model schematized in Figure 7, in which progression of CIS to invasive carcinoma is triggered by loss of Hh signaling. Following formation of CIS, the loss of *Shh* expression leads to decreased local expression of Hh-inducible stromal differentiation factors (BMPs), resulting in increased numbers of undifferentiated premalignant cells with proliferative advantages. Once transformed, these cells can then initiate focal invasive behavior, as they fail to elicit stromal differentiation factors (BMPs) while maintaining proliferative capacity. This proliferative advantage during progression to invasion results in selection of *Shh*-negative invasive carcinoma.

This model is strongly supported by the observed loss of *Shh* expression in both murine and human invasive urothelial carcinomas (Shin et al., 2014) (see Figure 1), and by the dramatically accelerated progression to invasive urothelial carcinoma observed with BBN exposure when stromal response to *Shh* signaling is experimentally ablated (see Figure 2). The role of BMPs as mediators of this effect is suggested by Shh-dependent expression of *BMP4* and *BMP5* in both murine and human stromal cells (Figures 3 and 4), and by the dramatically delayed progression to invasive carcinoma upon treatment with a BMP pathway agonist (Figure 5). We propose that this delay of progression is likely due to induction of urothelial cell differentiation by BMP pathway activity (Mysorekar et al., 2009); such activity is present in benign tissues and at early stages of tumor development because of stromal response to Shh from the urothelium. The local reduction or loss of this differentiation-inducing activity upon expansion of a clone of cells with loss of urothelial Shh expression might then permit tumor cells within a nascent microinvasion to continue to grow and advance, leading ultimately to invasive carcinoma (Figure 7). Interestingly, the TCGA study revealed that mutations of genes involved in epigenetic regulation were highly enriched in invasive urothelial carcinomas (Cancer Genome Atlas Research Network, 2014); these findings suggest the possibility that increased epigenetic plasticity may facilitate the loss of *SHH* expression during urothelial carcinoma progression.

DISCUSSION

The discovery of cyclopamine and synthetic mimics as Hh inhibitors that act by binding the essential pathway component *Smo* (Chen et al., 2002a, 2002b; Cooper et al., 1998; Incardona et al., 1998) has led to the development of potent *Smo*

Figure 6. Reduced Expression of Hedgehog and Bone Morphogenic Protein Pathway Ligands and Targets in Human Samples of Invasive Carcinoma as Compared to Normal Urothelium

RNA-seq data from TCGA database with annotation of samples based on published TCGA clusters (Cancer Genome Atlas Research Network, 2014). The y axis indicates $\log_2$-transformed fragments per kilobase of transcript per million mapped reads (FPKM) values normalized using the RSEM algorithm (Li and Dewey, 2011). If no reads map to the corresponding gene (FPKM = 0), the y axis value is set to −10. Note that for *SHH*, FPKM = 0 for 17/31 cluster 3 (basal) samples. Data are presented as mean and 95% confidence interval; normal: n = 19, cluster 1: n = 41, cluster 2: n = 42, cluster 3: n = 31, and cluster 4: n = 15; significance was calculated by Student's t test. See also Figure S5.

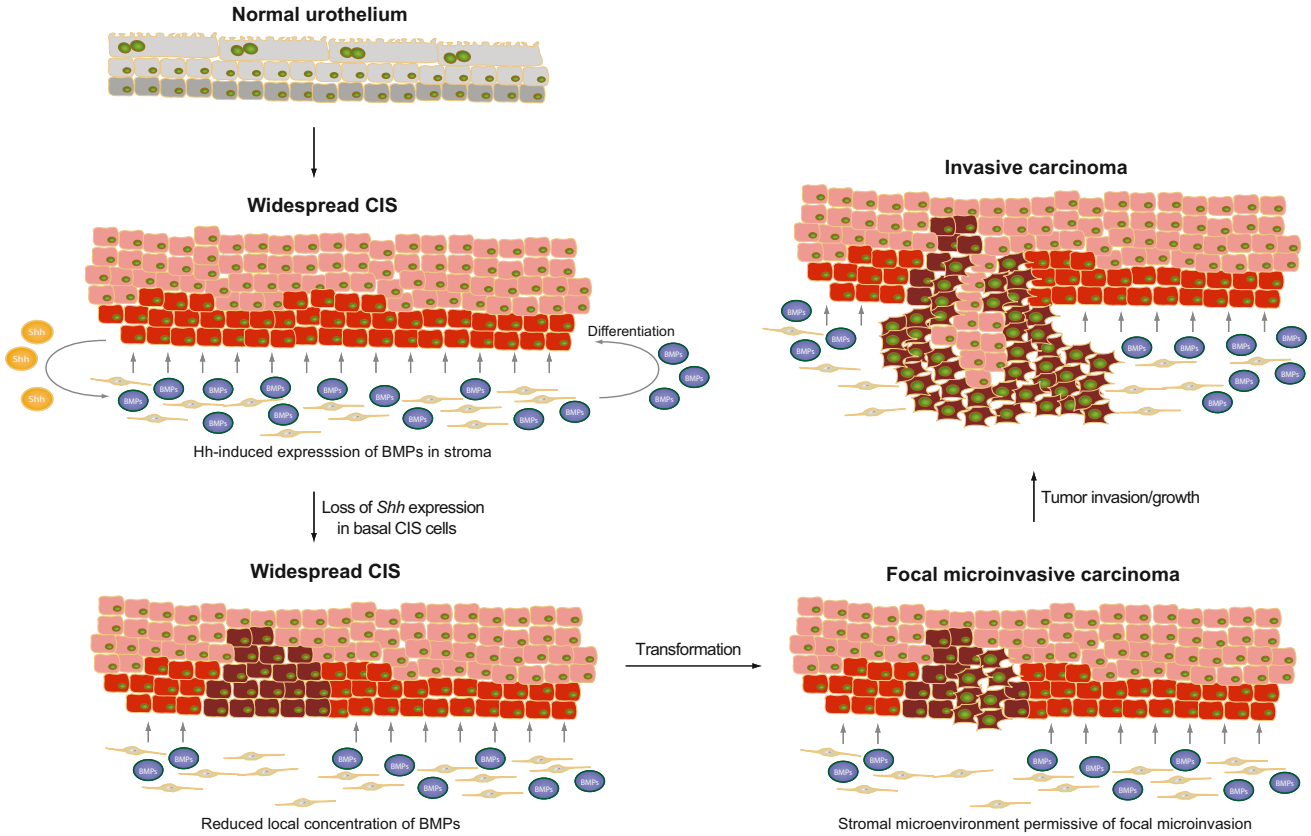

Figure 7. Model of Progression to Invasive Urothelial Carcinoma through Epithelial Loss of Hh Expression and Consequent Reduced Stromal Expression of Urothelial Differentiation Factors: Bone Morphogenic Proteins

CIS precursor lesion containing cells that express or do not express *Shh* (basal red and supra-basal pink cells, respectively) progresses to invasive carcinoma through clonal loss of *Shh* expression (brown cells) and expansion of a resulting invasive event. See text.

antagonists as therapeutic agents. One of these, Vismodegib, has been approved by the Food and Drug Administration for systemic use in patients with metastatic or locally advanced basal cell carcinoma (Ruch and Kim, 2013; Sekulic et al., 2012; Tang et al., 2012), and promising early results with this and other Hh inhibitors have been reported in clinical trials in medulloblastoma (Rudin et al., 2009). Despite promising preclinical studies in mice with xenografted or autochthonous tumors (Olive et al., 2009; Yauch et al., 2008), however, these drugs have not shown clinical benefit in trials of pancreatic, colon, or ovarian cancers (Herter-Sprie et al., 2013; Kaye et al., 2012; Ruch and Kim, 2013) and in some cases clinical trials had to be halted due to accelerated cancer progression (Herter-Sprie et al., 2013; Ruch and Kim, 2013).

Several recent papers, published during initial review of this manuscript, have indicated that stromal response to Hh signaling restrains the growth of oncogenic Kras-driven pancreatic cancer in mice (Lee et al., 2014; Özdemir et al., 2014; Rhim et al., 2014). These findings are more consistent with the results of pancreatic cancer clinical trials than the earlier preclinical studies, but do not reveal the molecular and cellular basis for these stromal effects. In addition, the reliance of these tumorigenesis models on expression of oncogenic Kras, which is associated with induction of *Shh* expression, leaves open the possibility that tumor-restraining effects of stromal Hh pathway response may be relevant primarily in the context of specific oncogene activation.

Our findings suggest that the restraining effects of stromal Hh response on cancer progression indeed may be more general because we have identified the urinary bladder as another organ of endodermal origin within which such an effect occurs. In addition, because the BBN-induced urothelial carcinoma model does not incorporate any prior genetic bias, the cancer-restraining effects of stromal Hh response apparently extend beyond Kras-dependent carcinogenesis to include other genetic etiologies. Our findings also identify Hh elicitation of differentiation-inducing BMP signals as the mechanism by which stromal Hh response restrains urothelial carcinoma progression; whether induction of differentiation by BMP or by other secreted factors mediates the tumor-restraining effect of Hh stromal response in pancreatic cancer and potentially other cancer types remains to be determined.

Although stromal response to Hh signaling in the context of the bladder includes expression of Wnt and other signals that trigger proliferation (Shin et al., 2011), our findings indicate that it is loss of differentiation-inducing factors such as Bmp4 and Bmp5 that is critical for cancer progression, raising the question as to the circumstances under which stromal induction of differentiation or proliferation may prevail as a critical factor. We know in the bladder that balanced production of proliferation- and

differentiation-inducing stromal signals is critical to regeneration of normal urothelium (Shin et al., 2011), but it seems that during cancer progression the differentiation-inducing activity becomes critical to keeping the tumor in check. A possible explanation for the heightened emphasis on differentiation factors is that cells of nascent epithelial cancers may first acquire reduced dependence on extracellular proliferative signals through genetic or epigenetic changes that generate cell-autonomous proliferative drive, while still leaving cells sensitive to the effects of stromal differentiation-inducing factors. This stromal source of differentiative drive may help confine proliferating cells to the epithelium, with cancer progression triggered by loss of the production or of the response to such stromal differentiation-inducing factors. If epithelial Hh signals to stroma in other endodermal organs also elicit balanced proliferative and differentiative responses, then an understanding of the impact of Hh pathway activity may require knowledge both of normal homeostasis as well as the derangements associated with carcinogenesis.

Finally, we note that our findings in urothelial carcinoma carry several significant therapeutic implications. First, because stromal Hh response may exert tumor-restraining effects in a wide range of cancers that originate from endodermal organs, careful evaluation and monitoring for the development of other malignancies would be important in patients undergoing systemic treatment with Hh pathway antagonists. Second, because FK506 treatment produces therapeutic BMP pathway activation at doses that cause minimal immunosuppression, such low-dose FK506 treatment may have utility in treatment of cancers arising from organs in which BMP pathway activity induces cellular differentiation. In bladder cancer, although ~70%–80% of cases present as noninvasive, high rates of recurrence and progression make treatment of this cancer more costly than any other on a per patient basis (Sievert et al., 2009). The ability to halt or slow progression by treatment with agents such as FK506 thus could have a significant beneficial impact on the clinical management of bladder cancer.

EXPERIMENTAL PROCEDURES

Mice

For *Smo* deletion experiments, *Gli1*$^{CreER/WT}$ mice were mated with the *Smo*$^{flox/flox}$ (Kimura et al., 2005; Long et al., 2001) strain to obtain *Gli1*$^{CreER/WT}$;*Smo*$^{flox/flox}$ and *Gli1*$^{CreER/WT}$;*Smo*$^{flox/WT}$ mice, which were injected intraperitoneally with 4 mg of TM (per 30 g body weight) daily for three consecutive days prior to BBN exposure. All mouse strains were obtained from Jackson Laboratories. Male mice 8–10 weeks of age were used. For each experiment, mice in each cage were randomly selected for drug/TM or control treatments. Mouse procedures were performed under isoflurane anesthesia, which was administered in a fume hood with a standard vaporizer (J.B. Baulch & Associates). All procedures were performed under a protocol approved by the Administrative Panel on Laboratory Animal Care at Stanford University.

N-butyl-N-4-hydroxybutyl Nitrosamine-Induced Bladder Carcinogenesis

A 0.1% concentration of BBN (TCI America) was dissolved in drinking water, and BBN-containing water was provided to mice *ad libitum* for 3–6 months in a dark bottle. BBN-containing water was changed twice a week. Bladders were collected and analyzed after 3 to 6 months of BBN administration.

Human Bladder Tissue Samples

Human bladder tissue samples were obtained from the Stanford Tissue Bank or were collected under appropriate informed consent agreements approved by the Institutional Review Board at Stanford University. The bladder tissue samples were obtained and processed within 1 hour after endoscopic resection or radical cystectomy from patients with confirmed muscle invasive urothelial carcinoma (stage $\geq$ pT2). For gene expression analysis, unfixed tissue samples were embedded in optimal cutting temperature (OCT) compound (Tissue-Tek) for snap freezing. For IHC, tissue samples were fixed in 4% paraformaldehyde (PFA) overnight at 4°C, followed by dehydrating in 30% sucrose overnight then embedded in OCT compound, and sectioned into 12-micron thick sections with a Microm cryostat.

Immunohistochemistry

Frozen sections of patient bladder tissue samples were air-dried for 20 min and postfixed in 4% PFA for 30 min. Sections were then blocked for endogenous peroxidase activity for 10 min with BLOXALL (Vector Labs) and subsequently incubated with 1.5% goat serum for 30 min, followed by incubation with primary rabbit anti-Shh antibody (C9C5, Cell Signaling) overnight. Sections were then incubated with secondary biotinylated goat antirabbit antibody (Vector Labs) for 60 min, followed by incubation with VECTSTAIN ABC Standard Kit (Rabbit IgG; Vector Labs) for 30 min. Sections were developed with ImmPACT DAB peroxidase substrate (Vector Labs) for 1 min and counterstained with Hematoxylin QS (Vector Labs). Sections were gradually dehydrated and cleared before mounting with cytoseal 60 (Thermo Scientific).

Histological Analysis

Human or mouse tissue specimens were embedded in OCT compound and sectioned into 12-micron thick sections with a Microm cryostat. Slides were fixed in 4% PFA for 30 min at 4°C, stained with hematoxylin, then counterstained with eosin. Histological assessment of bladder tissue sections was blinded in order to ensure that the pathologist who assessed the tissues did not know which treatment or patient group each sample belonged to.

Microarray Analysis

Gli1$^{CreER/WT}$;*Smo*$^{flox/flox}$ and *Gli1*$^{CreER/WT}$;*Smo*$^{flox/WT}$ mice were injected intraperitoneally with 4 mg of TM per 30 g body weight daily for three consecutive days. BBN-containing water was provided to the mice *ad libitum* after the last TM injection. After 2 months, the mice were sacrificed, bladders harvested, and total RNA was prepared using the RNeasy Plus Mini Kit (QIAGEN). RNA quality was evaluated using the Agilent 2100 Bioanalyzer system. Samples were hybridized to the Affymetrix GeneChip Mouse Exon 1.0 ST microarray chips. There were three mice of each genotype that were analyzed. After hybridization, expression values were normalized using the robust multiarray average function in the Partek Genomics Suite software. Differentially expressed genes were identified using ANOVA, genes showing a fold change greater or equal to two with p value < 0.01 were shortlisted for functional annotation analyses. Examination of overrepresented gene ontology terms and Swiss-Prot (SP) and Protein Information Resource (PIR) Keywords (SP_PIR_KEYWORDS) was performed using DAVID (Huang et al., 2007) (http://david.abcc.ncifcrf.gov/), in which enrichment in annotation terms was measured using a modified Fisher's Exact test. A p value < 0.05 was regarded as significant. Expression changes detected by microarray analysis were validated by verifying expression levels of several representative genes with quantitative RT-PCR.

Quantitative RT-PCR

Bladder samples were snap frozen in liquid nitrogen, homogenized with a mortar and pestle, and RNA extracted with the RNeasy Plus Mini kit (QIAGEN). For quantitative RT-PCR of mRNA transcripts, first-strand cDNA was made using the SuperScript III First-Strand Synthesis SuperMix (Invitrogen 18080-400). Quantitative RT-PCR was performed using iQ SYBR Green Supermix (Bio-Rad 170-8880) and the Bio-Rad iCycler, and gene expression was normalized to the house-keeping gene *HPRT1*.

Immunofluorescence Analysis

Bladders were harvested from mice, fixed in 4% PFA, embedded in OCT compound, and sectioned into 12-micron thick sections with a Microm cryostat. Sections were blocked in goat serum and incubated with primary antibodies (anti-SMA, Sigma 1A4, 1:1,000; anti-CD31, BD biosciences 550274, 1:500; and anti-EpCAM, Developmental Studies Hybridoma Bank G8.8, 1:500)

overnight at 4°C, washed, incubated with respective Alexa flor-conjugated antibodies, and imaged with a confocal microscope. For quantification of epithelial:stromal ratios, the total number of epithelial cells in each section, marked by expression of EpCAM, were counted. The total number of stromal cells, which are indicated by the nuclei present between the epithelial layer and the muscular bladder wall, were also counted and the ratio of the total number of epithelial cells to the total number of stromal cells in each tissue section calculated. For quantification of vascular density, the number of CD31+ vessels in four 40× fields of view per tissue section was counted and averaged to obtain the mean vascular density.

Human Bladder Cell Culture

Primary human bladder urothelial cells (ScienCell 4320) and bladder stromal fibroblasts (ScienCell 4330) were cultured in Urothelial Cell Medium (ScienCell 4321) and Fibroblast Medium (ScienCell 2301), respectively to subconfluency. Cells were then starved for 12 hr, followed by addition of Shh conditioned medium in the absence or in the presence of cyclopamine (3 μM, Toronto Research Chemicals), or treated with the Shh pathway agonist SAG (200 nM, Millipore) for 24 hr. In separate experiments, primary human bladder urothelial cells (ScienCell 4320) or J82 human urothelial carcinoma cells (American Type Culture Collection HTB1) were pretreated with 120 nM LDN-193189 or DMSO control (Selleckchem S2618) for 30 min prior to treatment with 20 ng/ml FK506 (Cayman Chemical) or treated with a DMSO control for 12 hr. Following treatment, RNA was extracted using the Trizol reagent.

Pump Implantation

Alzet osmotic pumps (Alzet, no. 2004) were used to administer FK506 (Cayman Chemical) to mice at a dose of 0.05 mg per kilogram mouse body weight per day. Each pump was filled with 200 μl of FK506, then implanted subcutaneously into the back of each mouse, slightly posterior to the scapulae, and the incision closed with wound clips.

Western Blotting

Control-treated or FK506-treated mouse bladders were homogenized and solubilized in radio-immunoprecipitation assay buffer, followed by brief centrifugation. Supernatants were utilized for SDS/PAGE and western blotting with phosphorylated Smad1/5/8 (Cell Signaling #9511) and control β-Actin (Santa Cruz sc-47778) antibodies. Densitometric analysis of western blot bands was performed using Image J software (NIH).

Data Analysis

Statistical analysis was performed using GraphPad Prism software v.5. All data are presented as mean ± SEM, and two group comparisons were done with a two-tailed Student's t test. A value of $p < 0.05$ was taken as statistically significant. For analysis of TCGA data, we downloaded bladder cancer (BLCA, Level 3) RNA-Seq data generated at University of North Carolina in IlluminaHiSeq_RNASeqV2 platform from the TCGA data portal. We annotated the data with the published TCGA bladder cancer clusters and normal bladder urothelium. We performed a t test to assess the significance.

ACCESSION NUMBERS

The microarray data are available in the Gene Expression Omnibus (GEO) database (http://www.ncbi.nlm.nih.gov/gds) under accession number GSE60654.

SUPPLEMENTAL INFORMATION

Supplemental Information includes five figures and two tables and can be found with this article online at http://dx.doi.org/10.1016/j.ccell.2014.09.001.

AUTHOR CONTRIBUTIONS

K.S and P.A.B. conceived ideas and experimental design. K.S., A.L., and C.Z. performed the experiments. D.S. analyzed data from the TCGA database. Y.P. and J.C.L. provided patient specimens and E.S provided advice on the use of FK506. K.S., A.L., and P.A.B. wrote the manuscript.

ACKNOWLEDGMENTS

This research was supported in part by grants from the NIH to P.A.B., and J.C.L. and a Pathway to Independence Award (K99/R00) to K.S. P.A.B. is an investigator of the Howard Hughes Medical Institute.

Received: May 2, 2014
Revised: July 14, 2014
Accepted: September 9, 2014
Published: October 13, 2014

REFERENCES

Ahn, S., and Joyner, A.L. (2005). In vivo analysis of quiescent adult neural stem cells responding to Sonic hedgehog. Nature *437*, 894–897.

Bragdon, B., Moseychuk, O., Saldanha, S., King, D., Julian, J., and Nohe, A. (2011). Bone morphogenetic proteins: a critical review. Cell. Signal. *23*, 609–620.

Bryan, G.T. (1977). The pathogenesis of experimental bladder cancer. Cancer Res. *37*, 2813–2816.

Bryan, G.T. (1983). Pathogenesis of human urinary bladder cancer. Environ. Health Perspect. *49*, 201–207.

Cancer Genome Atlas Research Network (2014). Comprehensive molecular characterization of urothelial bladder carcinoma. Nature *507*, 315–322.

Chen, J.K., Taipale, J., Cooper, M.K., and Beachy, P.A. (2002a). Inhibition of Hedgehog signaling by direct binding of cyclopamine to Smoothened. Genes Dev. *16*, 2743–2748.

Chen, J.K., Taipale, J., Young, K.E., Maiti, T., and Beachy, P.A. (2002b). Small molecule modulation of Smoothened activity. Proc. Natl. Acad. Sci. USA *99*, 14071–14076.

Choi, W., Porten, S., Kim, S., Willis, D., Plimack, E.R., Hoffman-Censits, J., Roth, B., Cheng, T., Tran, M., Lee, I.-L., et al. (2014). Identification of distinct basal and luminal subtypes of muscle-invasive bladder cancer with different sensitivities to frontline chemotherapy. Cancer Cell *25*, 152–165.

Cooper, M.K., Porter, J.A., Young, K.E., and Beachy, P.A. (1998). Teratogen-mediated inhibition of target tissue response to Shh signaling. Science *280*, 1603–1607.

Crabtree, G.R., and Schreiber, S.L. (2009). SnapShot: Ca2+-calcineurin-NFAT signaling. Cell *138*, 210–210.e211.

Cuny, G.D., Yu, P.B., Laha, J.K., Xing, X., Liu, J.-F., Lai, C.S., Deng, D.Y., Sachidanandan, C., Bloch, K.D., and Peterson, R.T. (2008). Structure-activity relationship study of bone morphogenetic protein (BMP) signaling inhibitors. Bioorg. Med. Chem. Lett. *18*, 4388–4392.

Hahn, H., Wicking, C., Zaphiropoulous, P.G., Gailani, M.R., Shanley, S., Chidambaram, A., Vorechovsky, I., Holmberg, E., Unden, A.B., Gillies, S., et al. (1996). Mutations of the human homolog of Drosophila patched in the nevoid basal cell carcinoma syndrome. Cell *85*, 841–851.

Herter-Sprie, G.S., Kung, A.L., and Wong, K.-K. (2013). New cast for a new era: preclinical cancer drug development revisited. J. Clin. Invest. *123*, 3639–3645.

Huang, W., Sherman, B.T., Tan, Q., Kir, J., Liu, D., Bryant, D., Guo, Y., Stephens, R., Baseler, M.W., Lane, H.C., and Lempicki, R.A. (2007). DAVID Bioinformatics Resources: expanded annotation database and novel algorithms to better extract biology from large gene lists. Nucleic Acids Res. *35*, W169–W175.

Incardona, J.P., Gaffield, W., Kapur, R.P., and Roelink, H. (1998). The teratogenic Veratrum alkaloid cyclopamine inhibits sonic hedgehog signal transduction. Development *125*, 3553–3562.

Johnson, R.L., Rothman, A.L., Xie, J., Goodrich, L.V., Bare, J.W., Bonifas, J.M., Quinn, A.G., Myers, R.M., Cox, D.R., Epstein, E.H., Jr., and Scott, M.P. (1996). Human homolog of patched, a candidate gene for the basal cell nevus syndrome. Science *272*, 1668–1671.

Kawai, S., and Sugiura, T. (2001). Characterization of human bone morphogenetic protein (BMP)-4 and -7 gene promoters: activation of BMP promoters by Gli, a sonic hedgehog mediator. Bone *29*, 54–61.

Kaye, S.B., Fehrenbacher, L., Holloway, R., Amit, A., Karlan, B., Slomovitz, B., Sabbatini, P., Fu, L., Yauch, R.L., Chang, I., and Reddy, J.C. (2012). A phase II, randomized, placebo-controlled study of vismodegib as maintenance therapy in patients with ovarian cancer in second or third complete remission. Clin. Cancer Res. *18*, 6509–6518.

Kimura, H., Stephen, D., Joyner, A., and Curran, T. (2005). Gli1 is important for medulloblastoma formation in Ptc1+/- mice. Oncogene *24*, 4026–4036.

Lai, K., Kaspar, B.K., Gage, F.H., and Schaffer, D.V. (2003). Sonic hedgehog regulates adult neural progenitor proliferation in vitro and in vivo. Nat. Neurosci. *6*, 21–27.

Lee, J.J., Perera, R.M., Wang, H., Wu, D.-C., Liu, X.S., Han, S., Fitamant, J., Jones, P.D., Ghanta, K.S., Kawano, S., et al. (2014). Stromal response to Hedgehog signaling restrains pancreatic cancer progression. Proceedings of the National Academy of Sciences *111*, E3091–E3100.

Li, B., and Dewey, C.N. (2011). RSEM: accurate transcript quantification from RNA-Seq data with or without a reference genome. BMC Bioinformatics *12*, 323–338.

Liu, J., Farmer, J.D., Jr., Lane, W.S., Friedman, J., Weissman, I., and Schreiber, S.L. (1991). Calcineurin is a common target of cyclophilin-cyclosporin A and FKBP-FK506 complexes. Cell *66*, 807–815.

Long, F., Zhang, X.M., Karp, S., Yang, Y., and McMahon, A.P. (2001). Genetic manipulation of hedgehog signaling in the endochondral skeleton reveals a direct role in the regulation of chondrocyte proliferation. Development *128*, 5099–5108.

Miyazono, K., and Miyazawa, K. (2002). Id: a target of BMP signaling. Sci. STKE *2002*, pe40.

Miyazono, K., Maeda, S., and Imamura, T. (2005). BMP receptor signaling: transcriptional targets, regulation of signals, and signaling cross-talk. Cytokine Growth Factor Rev. *16*, 251–263.

Mysorekar, I.U., Isaacson-Schmid, M., Walker, J.N., Mills, J.C., and Hultgren, S.J. (2009). Bone morphogenetic protein 4 signaling regulates epithelial renewal in the urinary tract in response to uropathogenic infection. Cell Host Microbe *5*, 463–475.

Nagao, M., Suzuki, E., Yasuo, K., Yahagi, T., and Seino, Y. (1977). Mutagenicity of N-butyl-N-(4-hydroxybutyl)nitrosamine, a bladder carcinogen, and related compounds. Cancer Res. *37*, 399–407.

O'Toole, C., Price, Z.H., Ohnuki, Y., and Unsgaard, B. (1978). Ultrastructure, karyology and immunology of a cell line originated from a human transitional-cell carcinoma. Br. J. Cancer *38*, 64–76.

Olive, K.P., Jacobetz, M.A., Davidson, C.J., Gopinathan, A., McIntyre, D., Honess, D., Madhu, B., Goldgraben, M.A., Caldwell, M.E., Allard, D., et al. (2009). Inhibition of Hedgehog signaling enhances delivery of chemotherapy in a mouse model of pancreatic cancer. Science *324*, 1457–1461.

Özdemir, B.C., Pentcheva-Hoang, T., Carstens, J.L., Zheng, X., Wu, C.-C., Simpson, T.R., Laklai, H., Sugimoto, H., Kahlert, C., Novitskiy, S.V., et al. (2014). Depletion of carcinoma-associated fibroblasts and fibrosis induces immunosuppression and accelerates pancreas cancer with reduced survival. Cancer Cell *25*, 719–734.

Palma, V., Lim, D.A., Dahmane, N., Sánchez, P., Brionne, T.C., Herzberg, C.D., Gitton, Y., Carleton, A., Alvarez-Buylla, A., and Ruiz i Altaba, A. (2005). Sonic hedgehog controls stem cell behavior in the postnatal and adult brain. Development *132*, 335–344.

Rhim, A.D., Oberstein, P.E., Thomas, D.H., Mirek, E.T., Palermo, C.F., Sastra, S.A., Dekleva, E.N., Saunders, T., Becerra, C.P., Tattersall, I.W., et al. (2014). Stromal elements act to restrain, rather than support, pancreatic ductal adenocarcinoma. Cancer Cell *25*, 735–747.

Roberts, D.J., Johnson, R.L., Burke, A.C., Nelson, C.E., Morgan, B.A., and Tabin, C. (1995). Sonic hedgehog is an endodermal signal inducing Bmp-4 and Hox genes during induction and regionalization of the chick hindgut. Development *121*, 3163–3174.

Roelink, H., Porter, J.A., Chiang, C., Tanabe, Y., Chang, D.T., Beachy, P.A., and Jessell, T.M. (1995). Floor plate and motor neuron induction by different concentrations of the amino-terminal cleavage product of sonic hedgehog autoproteolysis. Cell *81*, 445–455.

Ruch, J.M., and Kim, E.J. (2013). Hedgehog signaling pathway and cancer therapeutics: progress to date. Drugs *73*, 613–623.

Rudin, C.M., Hann, C.L., Laterra, J., Yauch, R.L., Callahan, C.A., Fu, L., Holcomb, T., Stinson, J., Gould, S.E., Coleman, B., et al. (2009). Treatment of medulloblastoma with hedgehog pathway inhibitor GDC-0449. N. Engl. J. Med. *361*, 1173–1178.

Samanta, J., and Kessler, J.A. (2004). Interactions between ID and OLIG proteins mediate the inhibitory effects of BMP4 on oligodendroglial differentiation. Development *131*, 4131–4142.

Schultheiss, T.M., Burch, J.B., and Lassar, A.B. (1997). A role for bone morphogenetic proteins in the induction of cardiac myogenesis. Genes Dev. *11*, 451–462.

Sekulic, A., Migden, M.R., Oro, A.E., Dirix, L., Lewis, K.D., Hainsworth, J.D., Solomon, J.A., Yoo, S., Arron, S.T., Friedlander, P.A., et al. (2012). Efficacy and safety of vismodegib in advanced basal-cell carcinoma. N. Engl. J. Med. *366*, 2171–2179.

Shin, K., Lee, J., Guo, N., Kim, J., Lim, A., Qu, L., Mysorekar, I.U., and Beachy, P.A. (2011). Hedgehog/Wnt feedback supports regenerative proliferation of epithelial stem cells in bladder. Nature *472*, 110–114.

Shin, K., Lim, A., Odegaard, J.I., Honeycutt, J.D., Kawano, S., Hsieh, M.H., and Beachy, P.A. (2014). Cellular origin of bladder neoplasia and tissue dynamics of its progression to invasive carcinoma. Nat. Cell Biol. *16*, 469–478.

Sievert, K.D., Amend, B., Nagele, U., Schilling, D., Bedke, J., Horstmann, M., Hennenlotter, J., Kruck, S., and Stenzl, A. (2009). Economic aspects of bladder cancer: what are the benefits and costs? World J. Urol. *27*, 295–300.

Spiekerkoetter, E., Tian, X., Cai, J., Hopper, R.K., Sudheendra, D., Li, C.G., El-Bizri, N., Sawada, H., Haghighat, R., Chan, R., et al. (2013). FK506 activates BMPR2, rescues endothelial dysfunction, and reverses pulmonary hypertension. J. Clin. Invest. *123*, 3600–3613.

Taipale, J., and Beachy, P.A. (2001). The Hedgehog and Wnt signalling pathways in cancer. Nature *411*, 349–354.

Tang, J.Y., Mackay-Wiggan, J.M., Aszterbaum, M., Yauch, R.L., Lindgren, J., Chang, K., Coppola, C., Chanana, A.M., Marji, J., Bickers, D.R., and Epstein, E.H., Jr. (2012). Inhibiting the hedgehog pathway in patients with the basal-cell nevus syndrome. N. Engl. J. Med. *366*, 2180–2188.

Teglund, S., and Toftgård, R. (2010). Hedgehog beyond medulloblastoma and basal cell carcinoma. Biochim. Biophys. Acta *1805*, 181–208.

Thievessen, I., Wolter, M., Prior, A., Seifert, H.H., and Schulz, W.A. (2005). Hedgehog signaling in normal urothelial cells and in urothelial carcinoma cell lines. J. Cell. Physiol. *203*, 372–377.

Weaver, M., Yingling, J.M., Dunn, N.R., Bellusci, S., and Hogan, B.L. (1999). Bmp signaling regulates proximal-distal differentiation of endoderm in mouse lung development. Development *126*, 4005–4015.

Yauch, R.L., Gould, S.E., Scales, S.J., Tang, T., Tian, H., Ahn, C.P., Marshall, D., Fu, L., Januario, T., Kallop, D., et al. (2008). A paracrine requirement for hedgehog signalling in cancer. Nature *455*, 406–410.

Yu, P.B., Deng, D.Y., Lai, C.S., Hong, C.C., Cuny, G.D., Bouxsein, M.L., Hong, D.W., McManus, P.M., Katagiri, T., Sachidanandan, C., et al. (2008). BMP type I receptor inhibition reduces heterotopic [corrected] ossification. Nat. Med. *14*, 1363–1369.